Personal Recognition Using Hand Shape and Texture

Ajay Kumar, *Member, IEEE*, and David Zhang, *Senior Member, IEEE*

***Abstract*—This paper proposes a new bimodal biometric system using feature-level fusion of hand shape and palm texture. The proposed combination is of significance since both the palmprint and hand-shape images are proposed to be extracted from the single hand image acquired from a digital camera. Several new hand-shape features that can be used to represent the hand shape and improve the performance are investigated. The new approach for palmprint recognition using discrete cosine transform coefficients, which can be directly obtained from the camera hardware, is demonstrated. None of the prior work on hand-shape or palmprint recognition has given any attention on the critical issue of feature selection. Our experimental results demonstrate that while majority of palmprint or hand-shape features are useful in predicting the subjects identity, only a small subset of these features are necessary in practice for building an accurate model for identification. The comparison and combination of proposed features is evaluated on the diverse classification schemes; naive Bayes (normal, estimated, multinomial), decision trees ($C4.5$, LMT), k-NN, SVM, and FFN. Although more work remains to be done, our results to date indicate that the combination of selected hand-shape and palmprint features constitutes a promising addition to the biometrics-based personal recognition systems.**

***Index Terms*—Biometrics, feature level fusion, feature subset selection and combination, hand-shape recognition, palmprint recognition.**

I. Introduction

MULTIMODAL biometric systems have recently attracted the attention of researchers and some work has already reported in the literature [1], [2], [5], [6]. Most of the reported work has been focused on bimodal biometric systems: fingerprint with face, face with iris, palmprint with face, fingerprint with face, or voice with face. With the notable exception of face and iris, these bimodal biometric systems use two different sensors or images to achieve the stated goals. The combination of iris and face investigated in [2] also use two different images. Such a combination would be highly popular if the iris images could be automatically extracted from the face images, which have been predominantly difficult/challenging due to the significant difference in imaging requirement of the two modalities. The palmprint and hand-shape information can be simultaneously extracted from a single image at medium resolution. Researchers have proposed several promising methods for palmprint [7], [10], [11] and hand-shape [30]–[33] recognition. However, there has not been any effort to combine these two modalities, which can be extracted from the single hand images, and this has been the focus of this work [3], [4].

The existing research on palmprint and hand-shape recognition or biometrics in general, has not made any attempt to evaluate the usefulness of the feature subset. Feature subset selection helps to identify and remove much of the irrelevant and redundant features. The small dimension of feature set reduces the hypothesis space, which is critical for the success of online implementation in personal recognition. These observations provide us the motivation to perform the experiments to illustrate the advantages of the feature subset selection for the examined palmprint and hand-shape features. Most of the prior work in the biometric fusion literature has examined the fusion of modalities at score level. However, the feature representation conveys the richest information as compared to the matching scores or abstract labels [5]. Therefore, the feature level fusion of hand-shape and palmprint features has been investigated.

A. Proposed Work

A personal recognition system that can simultaneously extract and utilize hand-shape and palmprint features is proposed. The advantages of the proposed system are twofold. First, the security threat associated with the hand-shape biometric, due to a fake hand, can be restricted with the integration of palmprint features. Second, a higher performance can be ensured due to the usage of bimodal features, which can be acquired from single hand image without any inconvenience to the users. The prior work on palmprint and hand-shape recognition has only emphasized on feature extraction and classification, and there has not been any attention on the critical issue of feature selection. Therefore, the goals of our experiments also include feature subset selection which is aimed to achieve similar or better performance with the usage of small number of features. We also performed rigorous experiments to evaluate the comparative performance of palmprint and hand-shape features on Bayes, support vector machines, feed-forward neural networks, k-nearest neighbor (NN), and decision-tree classifiers. In addition, the experiments reported in this paper are also aimed at; improving the performance of hand-shape recognition by exploring new features from the peg-free images; investigating the palmprint recognition in frequency domain using popular discrete cosine coefficients; and evaluating the performance gain from the feature subset selection and features combination.

The block diagram of the main steps involved in building the proposed biometric system is illustrated in Fig. 1. The hands images are acquired [3] from the digital camera and used to extract two distinct images: 1) binary image depicting hand shape

Manuscript received October 15, 2004; revised August 7, 2005. This work was supported in part by the CERG fund from the HKSAR Goverment, in part by the central fund from the Hong Kong Polytechnic University, and in part by the National Scientific Foundation of China (NSFC) under Contract 60332010. The associate editor coordinating the review of this manuscript and approving it for publication was Dr. Mario A. T. (G. E.) Figueiredo.

A. Kumar is with the Department of Electrical Engineering, Indian Institute of Technology Delhi, New Delhi 110016, India, and also with the Department of Computing, The Hong Kong Polytechnic University, Hung Hom, Kowloon, Hong Kong (e-mail: ajaykr@ieee.org).

D. Zhang is with the Department of Computing, The Hong Kong Polytechnic University, Hung Hom, Kowloon, Hong Kong (e-mail: csdzhang@comp.polyu.edu.hk).

Digital Object Identifier 10.1109/TIP.2006.875214

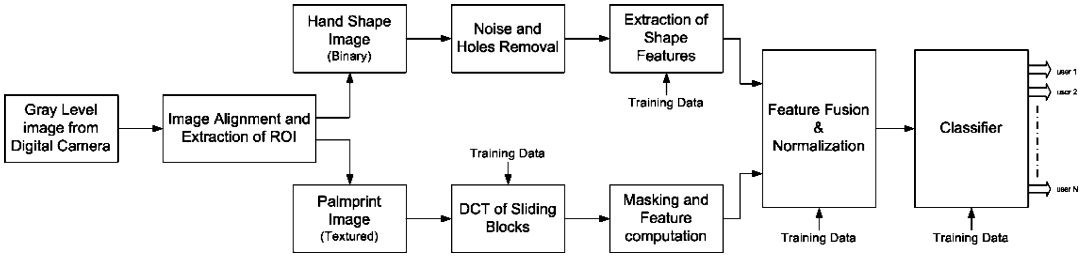

Fig. 1. Main steps involved in building the biometric system using hand shape and palmprint features.

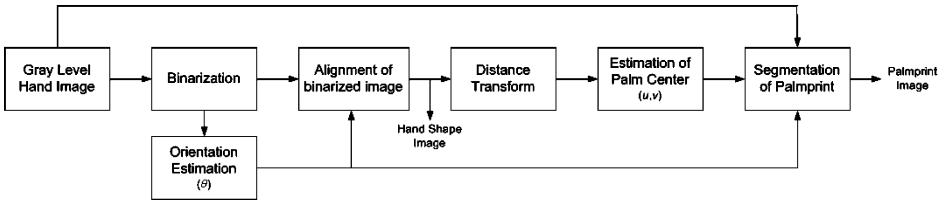

Fig. 2. Block diagram of automated extraction of two ROIs.

and 2) gray-level region of interest (ROI) depicting palmprint texture. Each of the extracted binary hand-shape images is further processed with morphological operations to remove any isolated small blobs or holes. The features extracted from palmprint and hand-shape images are concatenated and normalized before being fed to the classifier. One of the main differences of our approach from traditional approach is the inclusion of step that introduces feature subset selection, not shown in Fig. 1, is detailed in Section III. The experimental results are presented and discussed in Section V, which is followed by the conclusions of this paper in Section VI.

II. Automated Extraction of Hand-Shape and Palmprint Images

One of the crucial tasks in the proposed system is to extract two geometrically normalized images from a composite hand image acquired from the digital camera. The block diagram for the extraction of these two images, i.e., a binary image depicting hand-shape and a gray-level image containing palmprint texture, is shown in Fig. 2. Each of the acquired hand images are first subjected to thresholding operation to obtain the binarized image. The magnitude of thresholding limit η is computed by maximizing the object function $J_{op}(\eta)$, which denotes the measure of separablity between the two classes of pixels

$$J_{op}(\eta) = \frac{P_1(\eta)P_2(\eta)\left[\mu_1(\eta) - \mu_2(\eta)\right]}{\left[P_1(\eta) + P_2(\eta)\right]} \tag{1}$$

where the numbers of pixels in class 1 and 2 are represented by $P_1(\eta)$ and $P_2(\eta)$, $\mu_1(\eta)$ and $\mu_2(\eta)$ are the corresponding sample mean. The magnitude of η that maximizes $J_{op}(\eta)$ is selected [8] to be the thresholding value.

Each of the binarized hand-shape images is further aligned along the vertical direction as to restrict the feature variance due to the rotation. The orientation of each of the binarized image $P(x, y)$ is estimated by the parameters of the best-fitting ellipse [9]. The counterclockwise rotation of major axis relative to the normal axis is used to approximate the orientation θ

$$\theta = \begin{cases} \tan^{-1}\left(\dfrac{\rho_{11} - \rho_{22} + \sqrt{(\rho_{11} - \rho_{22})^2 + 4\rho_{12}^2}}{-2\rho_{12}}\right), & \text{if } \rho_{11} > \rho_{22} \\ \tan^{-1}\left(\dfrac{-2\rho_{12}}{\rho_{22} - \rho_{11} + \sqrt{(\rho_{22} - \rho_{11})^2 + 4\rho_{12}^2}}\right), & \text{otherwise} \end{cases} \tag{2}$$

where ρ_{11}, ρ_{22}, and ρ_{12} are the normalized second-order moments of pixels in the image $P(x, y)$ and (c_x, c_y) denote the location of its centroid

$$\rho_{11} = \frac{\sum\limits_{(x,y)\in P} (y - c_y)^2 . I(x, y)}{\sum\limits_{(x,y)\in S} I(x, y)}$$

$$\rho_{22} = \frac{\sum\limits_{(x,y)\in P} (x - c_x)^2 . I(x, y)}{\sum\limits_{(x,y)\in S} I(x, y)}, \text{ and}$$

$$\rho_{12} = \frac{\sum\limits_{(x,y)\in S} (y - c_y)(x - c_x) . I(x, y)}{\sum\limits_{(x,y)\in P} I(x, y)}. \tag{3}$$

The vertical alignment of the binarized hand-shape image is achieved by rotation matrix Ω, i.e.,

$$\Omega = \begin{bmatrix} \cos(\theta) & \sin(\theta) \\ \sin(\theta) & \cos(\theta) \end{bmatrix}. \tag{4}$$

The resultant geometrically normalized binary image may have isolated foreground blobs or holes. These artifacts are removed by morphological preprocessing, (Fig. 1) before the estimation of hand-shape features.

The distance transform of every pixel in the hand-shape image is used to estimate the center of palmprint. The location (u, v) of the pixel with highest magnitude of distance transform is obtained. All the gray-level pixels from the original hand

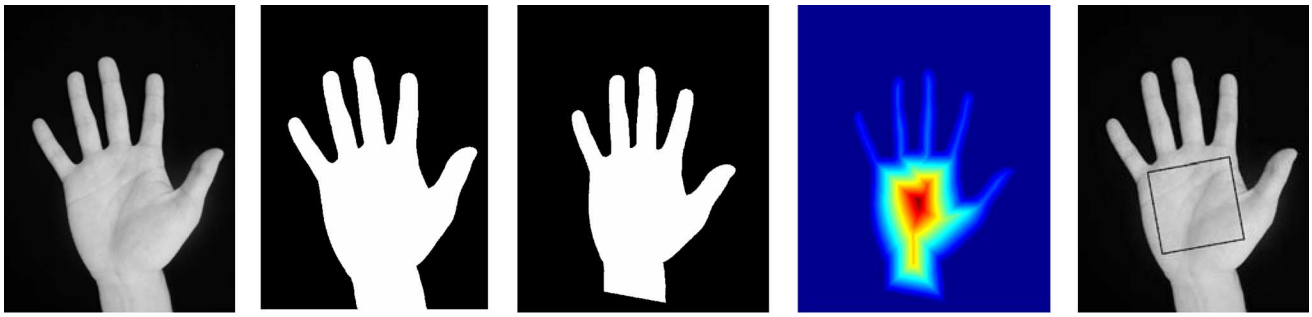

Fig. 3. (a) Acquired hand image. (b) Binarized hand-shape image used to extract the parameters of best-fitting ellipse. (c) Hand-shape image after rotation. (d) Distance transform of image. (e) Estimation of palmprint region using located center and orientation from (d) and (b), respectively. (Color version available online at http://ieeexplore.ieee.org.)

image, in a fixed-square region, centered at (u, v) and oriented along θ, are used as the palmprint image. The objective of set of operations detailed above is to achieve approximate translation, scale, and rotation invariance, and this is ensured as follows: translation invariance by the estimation of (u, v), scale invariance by fixed distance between camera and imaging board, and rotation invariance by the estimation of orientation θ. Fig. 3 shows the typical extraction of the hand-shape and palmprint image using the method described in this section.

A. Palmprint Features

The palmprint matching using texture-based [7], line-based [10], and appearance-based methods [11] have been proposed literature. The discrete cosine transform (DCT) has become one of the most successful transforms in image processing for the purpose of data compression, feature extraction, and recognition. The computational efficiency of the statistically sub-optimal transform is very high due to the various kind of fast algorithms [12] developed. However, the significance of DCT for palmprint images is yet to be investigated. The DCT that maps a $Q \times R$ spatial image block Ω to its values in frequency domain is defined as follows [13]:

$$T[x,y] = \varepsilon_x \varepsilon_y \sum_{q=0}^{Q-1} \sum_{r=0}^{R-1} \Omega_{qr} \cos \frac{\pi(2q+1)x}{2Q} \times \cos \frac{\pi(2r+1)y}{2R} \quad \begin{matrix} 0 \le x \le Q-1 \\ 0 \le y \le R-1 \end{matrix} \tag{5}$$

$$\text{where } \varepsilon_x = \begin{cases} 1/\sqrt{Q} & q = 0 \\ \sqrt{2/Q} & 1 \le q \le Q-1 \end{cases} \quad \text{and} \quad \varepsilon_y = \begin{cases} 1/\sqrt{R} & r = 0 \\ \sqrt{2/R} & 1 \le r \le R-1. \end{cases} \tag{6}$$

The palmprint image is divided into overlapping blocks of size $Q \times R$ as shown in Fig. 4(a). The DCT coefficients, i.e., $T[x, y]$ for each of these blocks are computed. Several of these DCT coefficients have values close to zero and can be discarded. In this work, all of the block DCT coefficients except those 12.5% coefficients shown in Fig. 4(b) are discarded. The feature vector from every palmprint image is formed by computing standard deviation of these significant DCT coefficients in each of these blocks.

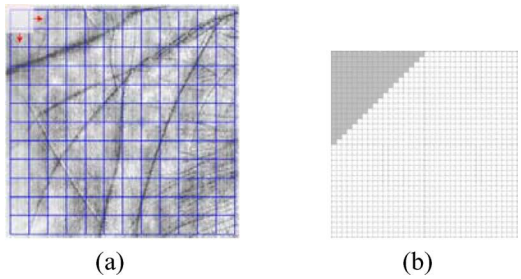

Fig. 4. (a) Computation of localized DCT coefficients in overlapping blocks. (b) Mask used to compute significant DCT coefficients from each of the blocks in (a). (Color version available online at http://ieeexplore.ieee.org.)

B. Hand-Shape Features

Hand-shape representation requires effective and perceptually important features based on geometrical information or geometry plus interior content. Shape is an important visual feature and has been used to describe and retrieve the image content [14], [15]. There are several shape properties that can be useful to describe and characterize the hand shape. However, there have not been any prior studies to examine these shape properties for hand-shape recognition. We investigated seven such shape properties, i.e., perimeter (f_1), solidity (f_2), extent (f_3), eccentricity (f_4), $x - y$ position of centroid relative to shape boundary $(f_5 - f_6)$, and convex area (f_7) to improve the success of prior methods. The definition and details of these features can be found in [15] and [16]. In addition, 16 geometrical features from the hand shape, as proposed in prior work [30]–[33], were also obtained; four finger length $(f_8 - f_{11})$, eight finger width $(f_{12} - f_{19})$, palm width (f_{20}), palm length (f_{21}), hand area (f_{22}), and hand length (f_{23}) (Fig. 5). Thus, each of the hand shape is characterized by a vector of 23 features. The signature analysis on the hand-shape boundary image is used to extract the image reference points, i.e., four fingertips, four interfinger points, and hand base, in a similar manner as detailed in [30]. The thumb features were not computed due to their poor reliability, as in [32], and its poor stability can be largely attributed to the peg-free imaging setup. All the feature distances are computed in terms of number of pixels in the binary image.

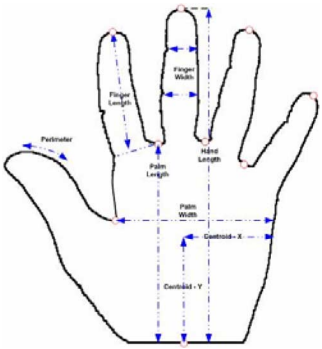

Fig. 5. Extraction of typical hand-shape features from the image of boundary pixels. (Color version available online at http://ieeexplore.ieee.org.)

III. Feature Evaluation and Selection

Several feature subset selection algorithms have been proposed in the literature. The wrapper is one of the most commonly used algorithms that evaluates and selects feature subset by repeated use of a particular classification algorithm. However, it is highly time consuming and prohibitive when the dimension of feature vectors is large (such as those from palmprints evaluated in this work). In this paper, we used the correlation-based feature selection (CFS) algorithm which has been shown [18] to be quite effective in feature subset selection. Unlike wrapper, CFS does not have to reserve a part of training data for evaluation which is difficult due to the limited availability of biometric training data. The CFS is a classifier-independent algorithm and its usefulness is illustrated from our experimental results. The CFS algorithm uses a correlation-based objective function to evaluate the usefulness of the features. The objective function $J_{\text{cfs}}(\lambda)$ is based on the heuristic that a good feature subset will have high correlation with the class label but will remain uncorrelated among themselves

$$J_{\text{cfs}}(\lambda) = \frac{\lambda \psi_{cr}}{\sqrt{\lambda + \lambda(\lambda - 1)\psi_{rr}}} \tag{7}$$

where ψ_{cr} is the average feature to class correlation and ψ_{rr} is the average feature to feature correlation within the class. The CFS-based feature selection algorithm uses $J_{\text{cfs}}(\lambda)$ to search the feature subsets using the best first search [19]. The search is aborted if the addition of new features does not show any improvement in the last five consecutive expanded combinations. We examined the usefulness of CFS scheme by evaluating recognition accuracy and the size of best feature subset with those from original feature set.

IV. Classification Schemes

Several classification algorithms to evaluate the performance and benefits of feature subset selection are investigated. These algorithms are quite popular and well known in pattern recognition literature [17]. However, with few notable exceptions, their usefulness for hand recognition is yet to be evaluated. The simplified version of Bayes rule, known as *naive Bayes*, which assumes that the feature vectors within a class are independent, was first evaluated. The *naive Bayes* has shown to work well with real data samples, and it traditionally makes the assumption that the feature values are normally distributed. However, this assumption may be violated in some domains and our experiments were not restricted to the normality assumption. The distribution of features was also estimated using nonparametric kernel density estimation [20] and employed in the *naive Bayes* classifier. The *multinomial* model [21] has been shown to outperform other alternative models on the real data and was, therefore, also investigated for the performance. The k-NN classifier employed minimum Euclidean distance between the query feature vector and all the prototype training data [23]. The support vector machine (SVM) [24] classifier employed polynomial kernel as it gave us the best results. The feed-forward neural network (FFN) employed a linear activation function for the last layer the sigmoid activation function was employed for other layers. The training weights were updated by using resilient backpropagation, which achieves faster convergence and conserves memory [25].

The $C4.5$ [26] decision tree is the most widely used algorithm and uses entropy criteria to select the most informative features for the branching during the training stage. The feature that gives the most information is selected to be at the root of the tree. Another extension of $C4.5$, also known as logistic model tree (LMT), uses a combination of tree structure and logistic regression model to build the decision tree. The different logistic regression functions at tree leaves are built using *LogitBoost* algorithm [22]. The construction of LMT is detailed in [27] and was evaluated in the experiments as it achieved much higher accuracy than $C4.5$.

V. Experiments and Results

In order to examine the goals of our experiments, the image database from 100 subjects was collected. The dataset consisted of 1000 images, ten images per subject, which were obtained from digital camera using unconstrained peg-free setup in indoor environment. These hand images were collected during two sessions with an average interval of three months, as the focus of experiments was to investigate the performance of biometric modalities instead of their stability with time. The volunteers were in the age group of 16–55 years but not very cooperative and were not paid for the data collection. During the image acquisition, the users were only required to make sure that 1) their fingers do not touch each other and 2) most of their hand (back side) touches the imaging table. The automated segmentation of hand-shape and palmprint image was achieved as detailed in Section II. Each of the 300 $\times$ 300 pixels segmented palmprint images were further divided into 24 $\times$ 24 pixels with an overlapping of six pixels as shown in Fig. 4(a). The feature vector of size 1 $\times$ 23 from hand shape and 1 $\times$ 144 from the palmprint image were initially extracted for the feature evaluation and selection from the training data. We employed five image samples from every user collected during the first session for training and the rest for testing. In order to allow fair comparison and combination of palmprint and hand-shape features, the same training and testing splits are used to generate the results.

The parameters of SVM and FFN employed in the experiments were empirically selected. The SVM using the nomial

TABLE I
COMPARATIVE PERFORMANCE EVALUATION FOR THE PALMPRINT RECOGNITION

	Naive Bayes			KNN	SVM			FFN	Decision Tree	
	Normal	*Estimated*	*Multinomial*		*d*=1	*d*=2	*d*=3		*C4.5*	*LMT*
144 Feature	69.4	74.4	91.8	94.4	95.2	95.8	95.8	95	50.6	94.6
69 features	68.8	75.4	92.8	95	94.4	95.6	95.5	94.8	50.2	93.8

TABLE II
COMPARATIVE PERFORMANCE EVALUATION FOR THE HAND-SHAPE RECOGNITION

	Naive Bayes			KNN	SVM			FFN	Decision Tree	
	Normal	*Estimated*	*Multinomial*		*d*=1	*d*=2	*d*=3		*C4.5*	*LMT*
23 Feature	73.9	79	29	84.6	89	88.4	88.6	86.4	67	89.6
15 Features	78.6	80	51.8	84.2	87	85.4	83.2	85	66.6	87.8

TABLE III
COMPARATIVE PERFORMANCE EVALUATION FOR THE COMBINED PALMPRINT AND HAND-SHAPE FEATURES

	Naive Bayes			KNN	SVM			FFN	Decision Tree	
	Normal	*Estimated*	*Multinomial*		*D*=1	*d*=2	*d*=3		*C4.5*	*LMT*
167 Feature	77	80	80.2	97.4	97.6	98	97.8	97.2	68.4	96
75 Features	78.2	78.6	94.2	97.8	97.8	97.8	98	96.8	68.2	96.4

kernel gave much better results than those from radial basis function. Therefore, to conserve the space, only results from polynomial kernel are reported. The SVM training was achieved with C-SVM, a commonly used SVM classification algorithm [28]. The training parameter γ and ε were empirically fixed at 1 and 0.001, respectively. Similarly, the number of input nodes in FFN were also empirically selected for the best performance; 100 (80) for palmprint, 50 (50) for hand shape, and 125 (75) for the combined feature set. The entries in the brackets represent the numbers when corresponding feature subset is employed for the performance evaluation. The FFN neuron weights were updated using resilient backpropagation algorithm and the training was aborted if the maximum number of training steps reached to 1000. The $C4.5$ decision tree was pruned with a confidence factor of 0.25. The splitting criteria for LMT was the same as the one used for $C4.5$, i.e., information gain. The minimum number of feature vectors at which a node can be considered for splitting was fixed to 15.

The experimental results for the palmprint recognition are summarized in Table I. This table also shows the performance of corresponding classifier with and without the feature subset selection. The evaluation of 144 palmprint features from the training set, using the CFS algorithm described in Section III, has revealed 75 redundant and irrelevant features. This suggests that the feature selection has been aggressively pursued in the palmprint domain. The performance of 69 relevant palmprint features, or feature subset, is also illustrated in Table I. It can be seen from this table that the kernel density *estimation* has managed to improve *naive Bayes* performance, but the performance improvement is significant when *multinomial* event model is employed. The best performance for palmprint recognition is achieved with SVM classifiers when the second order polynomial kernel is used. However, the achieved performance of nearest neighbor classifier suggest that it may be preferred in some applications as it is inherently simple and does not require

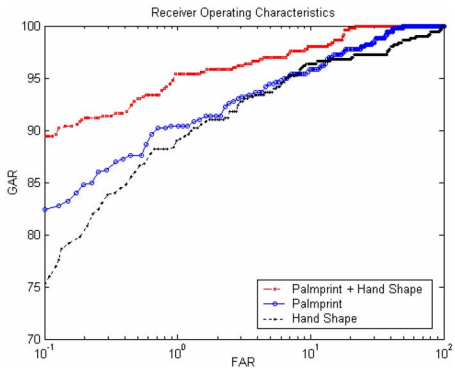

Fig. 6. Receiver operating characteristics using from the hand-shape and palmprint features. (Color version available online at http://ieeexplore.ieee.org.)

training phase. The performance of FFN is better than *naive Bayes*, but quite similar to that of SVM or k-NN. The performance of decision tree $C4.5$ has been worst and this may be due to the large number of features that make the repeated portioning of data difficult. However, the performance of LMT is also promising and similar to that of k-NN. The average tree size for the decision tree build using 144(51) features for LMT and $C4.5$ was 16 (12) and 285 (281), respectively. This is not surprising as LMT algorithm has shown [27] to be often more accurate than $C4.5$ and always resulting in a tree of small size than those from $C4.5$.

One of the important conclusions from Table I is that the usage of feature selection has effectively reduced the number of features by 52.08% while improving or maintaining similar performance in most cases. *This suggests that, while the majority of palmprint (DCT) features are useful in predicting the subjects identity, only a small subset of these features are necessary, in practice, for building an accurate model for identification.*

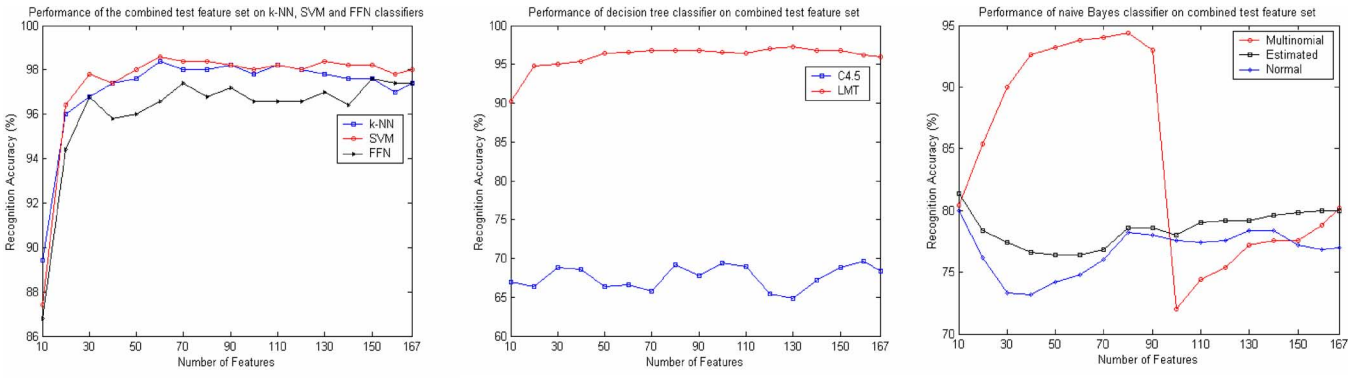

Fig. 7. Prformance analysis of classifiers with the number of features; k-NN, SVM, and FFN in (a), decision trees in (b), and naive Bayes in (c). (Color version available online at http://ieeexplore.ieee.org.)

Table II summarizes the experimental results for the hand-shape identification. The evaluation of 23 hand-shape features from the training data has selected 15 most informative features; f_1, f_7, $f_8 - f_{11}$, f_{14}, $f_{16} - f_{19}$, and $f_{20} - f_{23}$. The decision tree using LMT achieved the best performance while those from the *multinomial naive Bayes* is the worst. The usage of the *multinomial* event model in *naive Bayes* has resulted in significant performance improvement from the palmprint features (Table I) while the usage from hand-shape features has been degraded (Table II). This can be attributed to the inappropriate estimation [29] of the term probabilities resulting from the small size hand-shape feature vectors. The average size of decision tree build using 23 (15) features using LMT and $C4.5$ was 81 (69) and 251 (255), respectively.

The experimental results for the combined hand-shape and palmprint features are shown in Table III. The CFS algorithm selected 75 features subset from the combined list of 167 features. The combined feature subset had 13 hand-shape features, i.e., f_3, f_7, f_8, $f_{10} - f_{14}$, $f_{17} - f_{18}$, $f_{20} - f_{23}$, and 62 palmprint features. It may be noted that the reduced feature subset obtained from the combined feature set is not the addition or sum of reduced feature subsets individually obtained from palmprint and hand-shape feature sets. *This suggests that only a certain combination of features, rather than the combination of individual feature subsets carrying the discriminatory information, is useful in the feature level fusion*. The new hand-shape features selected in the individual and combined feature subsets, i.e., f_3, f_3, and f_7, justify their usefulness. However, other new examined hand-shape features, i.e., f_2, f_4, f_5, and f_6, could not establish their significance. As shown in Table III, the SVM classifier achieved the best performance which is closely followed by k-NN. It can be noted that the combination of hand-shape and palmprint features has been useful in improving the performance for all the classifiers except for the case from *naive Bayes* classifier. The performances of combined features from the *multinomial naive Bayes* classifier using feature subset selection suggests that the *multinomial* event model is most sensitive to irrelevant and redundant features. The size of decision tree build using 147 (100) features using LMT and $C4.5$ was 16 (12) and 285 (231), respectively. The best results for k-NN are obtained when $k = 1$ and has been used in Tables I–III. We also performed the experiments using the k-NN classifier to ascertain the performance for user authentication. Fig. 6 shows the receiver operating characteristics from the respective features and their feature-level fusion.

It is prudent to examine how the performance of various classifiers is adversely affected by the irrelevant and redundant features. The performance improvement of these classifiers with the availability of more features, using a fixed number of training samples, is investigated. In this set of experiments, all the available features from the training samples were ranked in the order of their merit using CFS objective functions (6). The feature vectors in the test data set were also ranked in the same order of ranking generated from the training data. The performance of these classifiers starting from first ten features was computed and the next ten features were added at every successive iterations. The number of input nodes for FFN classifier was empirically fixed to 75, irrespective of number of features. Fig. 7(a) shows the performance variation for k-NN, SVM, and FFN classifiers with the increase in number of features. The SVM classifier does not show any appreciable increase in the performance with the addition of irrelevant features (say beyond 75) and its performance is generally the best of all the classifiers evaluated in this paper. *It is interesting to note that the feature selection strategy has been able to find 20 (10) best features that give ≈96% (89%) accuracy using the SVM classifier. This 20(10) feature subset consists of 15(6) palmprint and 5 (4) hand-shape features*.

The performance of the LMT classifier in Fig. 7(b) shows an initial increase in performance with the increase in informative features, but the performance stabilizes with the addition of noninformative and redundant features (beyond 70-75). Thus, the performance of LMT suggests that it is insensitive to the redundant and irrelevant features, and this is due to the fact that the LMT is built using the stagewise fitting process to construct the logistic regression models which select only relevant features from the training data. The $C4.5$ decision tree continues to maintain worse performance and the feature selection strategy do not have any appreciable effect on the performance. Fig. 7(c) shows the results for the performance of *naive Bayes* classifier. The performance estimates of the *naive Bayes multinomial* classifier shows a tendency of exponential increase with a small

number of features before an abrupt decrease in performance. The performance of the *naive Bayes* with nonparametric kernel estimation is marginally better than those with *normal* assumption, but is still quite poor.

VI. Conclusion

This paper introduces a new bimodal personal authentication system by integrating hand-shape and palmprint features, simultaneously acquired from the single hand image. The proposed method of hand-shape and palmprint image segmentation, and the combination of features from these two images, has shown to be useful in achieving higher performance. It is not possible to locate the relevant features from the real biometrics data in advance, and, therefore, the performance of feature selection strategy must be measured indirectly. The best way to do this is to compare the classifier performance with and without feature subset selection. The performance of palmprint and hand-shape features, and the effectiveness of feature subset selection, was evaluated on the diverse classification schemes, probabilistic classifier (naive Bayes), decision tree classifier ($C4.5$, LMT), and instance-based classifier (k-NN), and learned classifiers (SVM, FFN). Our experimental results in Section V suggested the usefulness of shape properties (e.g., perimeter, extent, convex area) which can be effectively used to enhance the performance in hand-shape recognition. Similarly, the proposed approach for the palmprint recognition using DCT coefficients has also shown promising results. *This investigation is useful as the DCT coefficients can be directly obtained from the camera hardware using commercially available DCT chips that can perform fast and efficient DCT transforms*.

Experimental studies in this paper further suggest that, while a majority of features extracted from the hand images are useful in subject recognition, only a small subset of these features are actually needed in practice for building an accurate model for subject recognition. This is important, as none of the prior studies on palmprint, hand-shape, or fusion literature has focused on the issue of feature subset selection. The usage of small size feature vectors results in reduced computational complexity, which is critical for online personal recognition. The analysis of experimental results in Tables I–III suggests that the correlation-based feature subset selection is capable of effectively selecting the relevant palmprint and hand-shape features. *Although more work remains to be done, our results to date indicate that the combination of hand-shape and palmprint features constitutes a promising addition to the biometrics-based personal recognition systems*.

References

[1] L. Hong and A. Jain, "Integrating faces and fingerprints for personal identification," *IEEE Trans. Pattern Anal. Mach. Intell.*, vol. 20, no. 12, pp. 1295–1307, Dec. 1998.

[2] Y. Wang, T. Tan, and A. K. Jain, "Combining face and iris for identity verification," in *Proc. AVBPA*, Guildford, U.K., Jun. 2003, pp. 805–813.

[3] A. Kumar and D. Zhang, "Biometric recognition using feature selection and combination," in *Proc. AVBPA*, New York, Jul. 2005, pp. 813–822.

[4] A. Kumar, D. C. M. Wong, H. Shen, and A. K. Jain, "Personal verification using palmprint and hand geometry biometric," in *Proc. AVBPA*, Guildford, U.K., Jun. 2003, pp. 668–675.

[5] A. K. Jain, A. Ross, and S. Prabhakar, "An introduction to biometric recognition," *IEEE Trans. Circuits Syst. Video Technol.*, vol. 14, no. 1, pp. 4–20, Jan. 2004.

[6] K.-A. Toh and W.-Y. Yau, "Combination of hyperbolic functions for multimodal biometrics data fusion," *IEEE Trans. Syst. Man, Cybern. B, Cybern.*, vol. 34, no. 2, pp. 1196–1209, Apr. 2004.

[7] D. Zhang, W. K. Kong, J. You, and M. Wong, "On-line palmprint identification," *IEEE Trans. Pattern Anal. Mach. Intell.*, vol. 25, no. 9, pp. 1041–1050, Sep. 2003.

[8] N. Otsu, "A threshold selection method from gray-scale histogram," *IEEE Trans. Syst., Man, Cybern.*, vol. 8, no. 1, pp. 62–66, Jan. 1978.

[9] R. M. Haralick and L. G. Shapiro, *Computer Vision and Robot Vision*. Reading, MA: Addison-Wesley, 1991.

[10] D. Zhang and W. Shu, "Two novel characteristics in palmprint verification: datum point invariance and line feature matching," *Pattern Recognit.*, vol. 32, no. 4, pp. 691–702, Apr. 1999.

[11] X. Lu, D. Zhang, and K. Wang, "Fisherpalms based palmprint recognition," *Pattern Recognit. Lett.*, vol. 24, pp. 2829–2838, Nov. 2003.

[12] Wang, Z. He, C. Zou, and J. D. Z. Chen, "A generalized fast algorithm for n-D discrete cosine transform and its application to motion picture coding," *IEEE Trans. Circuits Syst. II, Exp. Briefs*, vol. 46, no. 5, pp. 617–627, May 1999.

[13] A. K. Jain, *Fundamentals of Digital Image Processing*. Englewood Cliffs, NJ: Prentice-Hall, 1989.

[14] D. Zhang and G. Lu, "Review of shape representation and description techniques," *Pattern Recognit.*, vol. 37, pp. 1–19, 2004.

[15] O. El. Badawy and M. Kamel, "Shape-based image retrieval applied to trademark images," *Int. J. Image Graph.*, vol. 2, no. 3, pp. 375–393, 2002.

[16] J. C. Russ, *The Image Processing Handbook*, 3rd ed. Boca Raton, FL: CRC, 1999.

[17] I. H. Witten and E. Frank, *Data Mining: Practical Machine Learning Tools and Techniques With Java Implementations*. San Mateo, CA: Morgan Kaufman, 1999.

[18] M. A. Hall and L. A. Smith, "Practical feature subset selection for machine learning," in *Proc. 21st Australian Computer Science Conf.*, 1998, pp. 181–191.

[19] M. A. Hall, "Correlation-based feature selection for discrete and numeric class machine learning," presented at the 7th Int. Conf. Machine Learning, Stanford, CA, 2000.

[20] G. H. John and P. Langley, "Estimating continious distribution in Bayesian classifiers," presented at the 11th Conf. Uncertainty in Artificial Intelligence, 2000.

[21] A. McCallum and K. Nigam, "A comparison of event model for naive Bayes text classification," presented at the AAAI Workshop on Learning for Text Categorization, 1998.

[22] J. Friedman, T. Hastie, and R. Tibshirani, "Additive logistic regression: a statistical view of boosting," *Ann. Statist.*, vol. 38, no. 2, pp. 337–374, 2000.

[23] D. W. Aha, D. Kibler, and K. Albert, "Instance based learning algorithms," *Mach. Learn.*, vol. 6, pp. 37–66, 1991.

[24] V. Vapnik, *Statistical Learning Theory*. New York: Wiley, 1998.

[25] M. Riedmiller and H. Braun, "A direct adaptive method for faster backpropagation learning: the PROP algorithme," in *Proc. Int. Conf. Neural Networks*, Apr. 1993, vol. 1, pp. 586–591.

[26] R. Quinlan, *C4.5: Programs for Machine Learning*. San Mateo, CA: Morgan Kaufman, 1993.

[27] N. Landwehr, M. Hall, and E. Frank, "Logistic model trees," in *Proc. 14th Eur. Conf. Machine Learning*, 2003, vol. 2837, pp. 241–252.

[28] N. Cristianini and J. S. Taylor, *An Introduction to Support Vector Machines*. Cambridge, U.K.: Cambridge Univ. Press, 2001.

[29] S.-B. Kim, H.-C. Rim, and H.-S. Lim, "A new method of parameter estimation for multinomial naive Bayes text classifiers," in *Proc. SIGIR*, Tampere, Finland, Aug. 11–15, 2002, pp. 391–392.

[30] C. Oden, A. Ercil, and B. Buke, "Combining implicit polynomials and geometric features for hand recognition," *Pattern Recognit. Lett.*, vol. 24, pp. 2145–2152, 2003.

[31] A. K. Jain, A. Ross, and S. Pankanti, "A prototype hand geometry-based verification system," in *Proc. AVBPA*, Washington, DC, 1999, pp. 166–171.

[32] R. Sanchez-Reillo, C. Sanchez-Avila, and A. Gonzales-Marcos, "Biometric identification through hand geometry measurements," *IEEE Trans. Pattern Anal. Mach. Intell.*, vol. 22, no. 10, pp. 1168–1171, Oct. 2000.

[33] A. Ross and A. K. Jain, "Information fusion in biometrics," *Pattern Recognit. Lett.*, vol. 24, pp. 2115–2125, Sep. 2003.

Ajay Kumar (M'99) received the Ph.D. degree from The University of Hong Kong in May 2001, where he completed his doctoral research in a record time of 21 months (September 1999 to May 2001).

He was with the Indian Institute of Technology (IIT), Kanpur, as a Junior Research Fellow and at IIT Delhi, New Delhi, as a Senior Scientific Officer before joining Indian Railways. He joined the Indian Railway Service of Signal Engineers (IRSSE) in 1993 and was an Assistant Signal and Telecom Engineer. He was a Project Engineer at IIT Kanpur from 1996 to 1997 and an Assistant Professor at NIST, Berhampur, India, from September 1997 to September 1998. He was a Research Associate with The University of Hong Kong from December 1998 to August 1999. He did his postdoctoral research at the Department of Computer Science, Hong Kong University of Science and Technology, Kowloon, from October 2001 to December 2002. He was awarded The Hong Kong Polytechnic University Postdoctoral Fellowship for 2003 to 2005, where he was with the Department of Computing from April 2004 to February 2005. Currently, he is a faculty member with the Department of Electrical Engineering, IIT Delhi. His research interests include pattern recognition with the emphasis on biometrics and defect detection using wavelets, general texture analysis, neural networks, and support vector machines.

David Zhang (SM'95) received the degree in computer science from Peking University, Peking, China, in 1974, the M.Sc. and Ph.D. degrees in computer science and engineering from the Harbin Institute of Technology (HIT), Harbin, China, in 1983 and 1985, respectively, and the Ph.D. degree in electrical and computer engineering from the University of Waterloo, Waterloo, ON, Canada, in 1994.

From 1986 to 1988, he was a Postdoctoral Fellow at Tsinghua University, China, and then became an Associate Professor at Academia Sinica, Beijing, China. Currently, he is a Professor at The Hong Kong Polytechnic University, Kowloon. He also serves as an Adjunct Professor at Tsinghua University; Shanghai Jiao Tong University, China; HIT; and the University of Waterloo. His research interests include automated biometrics-based authentication, pattern recognition, and biometric technology and systems. He is the Founder and Director of both the Biometrics Research Centers at The Hong Kong Polytechnic University and HIT, supported by UGC/CRC, the Hong Kong Government, and the National Scientific Foundation of China (NSFC), respectively. He has published over 180 articles, including seven books in his research areas.

Dr. Zhang is the Founder and Editor-in-Chief of the *International Journal of Image and Graphica* and an Associate Editor of the IEEE TRANSACTIONS ON SYSTEMS, MAN, AND CYBERNETICS—PART A: SYSTEMS AND HUMANS, the IEEE TRANSACTIONS ON SYSTEMS, MAN, AND CYBERNETICS—PART C: APPLICATIONS AND REVIEWS, *Pattern Recognition*, the *International Journal of Pattern Recognition and Artificial Intelligence*, *Information: International Journal*, and the *International Journal of Robotics and Automation and Neural, Parallel, and Scientific Computations*.